Langmuir

Article

pubs.acs.org/Langmuir

Surface Modification of Poly(dimethylsiloxane) Using Ionic Complementary Peptides to Minimize Nonspecific Protein Adsorption

Xiaoling Yu, Junzhu Xiao, and Fuquan Dang*

Key Laboratory of Analytical Chemistry for Life Science of Shaanxi Province, School of Chemistry and Chemical Engineering, Shaanxi Normal University, 620 West Chang'an Street, Xi'an 710119, China

Supporting Information

ABSTRACT: Poly(dimethylsiloxane) (PDMS) has become a widely used material for microfluidic and biological applications. However, PDMS has unacceptably high levels of nonspecific protein adsorption, which significantly lowers the performance of PDMS-based microfluidic chips. Most existing methods to reduce protein fouling of PDMS are to make the surface more hydrophilic by surface oxidization, polymer grafting, and physisorbed coatings. These methods suffer from the relatively short-term stability, the multistep complex treatment procedure, or the insufficient adsorption reduction. Herein, we developed a novel and facile modification method based on self-assembled peptides with well-tailored amino acid composition and sequence, which can also interact strongly with the PDMS surface in the same way as proteins, for suppressing the nonspecific protein fouling and improving the biocompatibility of PDMS-based microfluidic chips. We first demonstrated that an ionic complementary peptide, EAR16-II with a sequence of $[(Ala\text{-}Glu\text{-}Ala\text{-}Glu\text{-}Ala\text{-}Arg\text{-}Ala\text{-}Arg)_2]$, can readily self-assemble into an amphipathic film predominantly composed of tightly packed β-sheets on the native hydrophobic and plasma-oxidized hydrophilic PDMS surfaces upon low concentrations of carbohydrates. The self-assembled EAR16-II amphipathic film exposed its hydrophobic side to the solution and thus rendered the PDMS surface hydrophobic with water contact angles (WCAs) of around 110.0°. However, the self-assembled EAR16-II amphipathic film exhibited excellent protein-repelling and blood compatibility properties comparable to or better than those obtained with previously reported methods. A schematic model has been proposed to explain the interactions of EAR16-II with the PDMS surface and the antifouling capability of EAR16-II coatings at a molecular level. The current work will pave the way to the development of novel coating materials to address the nonspecific protein adsorption on PDMS, thereby broadening the potential uses of PDMS-based microfluidic chips in complex biological analysis.

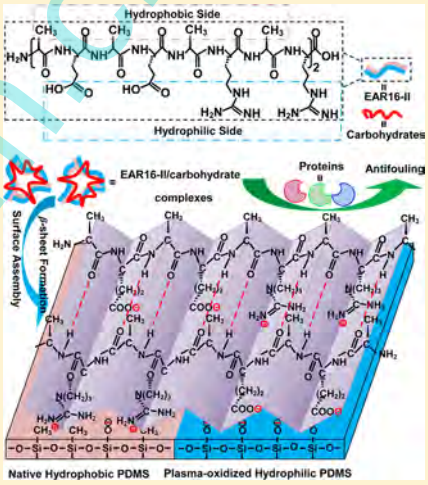

INTRODUCTION

In the past two decades, polydimethylsiloxane (PDMS) has been widely adopted for the fabrication of microfluidic chips due to its excellent features, including chemical inertness, elastomeric properties, nontoxicity, gas permeability, optical transparency, and ease of fabrication.[1−4] Currently, PDMS-based microfluidic chips have been extensively used in many applications including clinical diagnostics, high-throughput screening, genetic research, protein analysis, cell analysis, and biosensing.[5−10] However, the hydrophobic surface of PDMS with a heterogeneous surface charge often results in poor wetting with aqueous media, nonspecific adsorption of analytes, and unstable electroosmotic flow (EOF). These disadvantages lead to substantial sample loss and poor performance of PDMS-based microfluidic chip, for example, the relatively low separation efficiency of microchip electrophoresis (MCE). Therefore, the surface chemistry of PDMS often demands further modification to successfully use PDMS-based microfluidic chips in biological applications.[11−13]

Various strategies have been explored to improve the wettability, biocompatibility, and antifouling properties of microfluidic chips; these include plasma and UV oxidation,[14,15] chemical modification,[16−20] and dynamic coating.[21−24] The majority of these techniques have been developed for electrophoresis applications because channel surface properties critically affect separation performance. However, challenges in surface modification with plasma oxidation remain due to fast hydrophobic recovery of PDMS by reorientation of hydroxyl groups from the surface to the polymer bulk or migration of hydrophobic low molar mass PDMS residues to the surface.[14,15,25] Physical damage can occur to the PDMS surface, and limited biocompatibility is obtained after chemical modification that is a multistep process and difficult to achieve because of chemical inert PDMS.[16,17] In contrast, dynamic coatings represent a simple and extensively used method, in

Received: March 26, 2015
Revised: May 7, 2015
Published: May 12, 2015

DOI: 10.1021/acs.langmuir.5b01085
Langmuir 2015, 31, 5891−5898

which the coating layers are easier to apply and regenerate; the coating often requires only a simple rinse of the surface of interest with a solution of coating additives. Nonspecific adsorption of analytes can be effectively passivated by a coating layer of surfactants and water-soluble polymers physically preabsorbed on the channel wall. However, a disadvantage of dynamic coatings is the potentially weak interactions of coating additives with the surface, which may lead to unstable coatings and even undesired nonspecific adsorption of analytes, especially proteins. Therefore, using dynamic coatings to fabricate stable protein-repelling PDMS surfaces still remains challenging.[11,12,21]

Recently, a special class of self-assembling peptides with alternating hydrophobic and hydrophilic residues has drawn much attention because of their intrinsic tendency to adopt β-sheet conformations, showing great potential in a wide range of applications including tissue scaffolding, biological surface patterning, regenerative medicine, and drug delivery.[26−29] Among them, an ionic complementary peptide EAK16-II [(Ala-Glu-Ala-Glu-Ala-Lys-Ala-Lys)$_2$], originally from a yeast z-DNA binding protein,[30] is of special interest. EAK16-II contains amino acid residues involved in a variety of molecular interactions in proteins, including hydrogen bonding, electrostatic, and hydrophobic interactions. In addition, the alternation of hydrophobic (alanine, A) and hydrophilic (glutamic acid, E, and lysine, K) residues provides the amphipathic property for EAK16-II with hydrophobic and charged residues positioned in the opposite directions. This amino acid sequence allows the peptide to self-assemble into unusually stable β-sheet-rich nanofibrils and macroscopic membranes in solution.[30,31] Such unique properties suggest that ionic complementary peptides can potentially be used as highly efficient coating additives for minimizing nonspecific protein adsorption on a PDMS surface.

In the current work, an ionic complementary peptide EAR16-II [(Ala-Glu-Ala-Glu-Ala-Arg-Ala-Arg)$_2$], which has higher surface activity than EAK16-II based on our preliminary experiments, was designed and synthesized as a novel coating additive for improving the antifouling and biocompatibility properties of PDMS-based microfluidic chips. The self-assembly of EAR16-II on both native hydrophobic and plasma-oxidized hydrophilic PDMS surfaces was comprehensively characterized by various techniques including atomic force microscopy (AFM), water contact angle (WCA), attenuated total reflection Fourier transform infrared spectroscopy (ATR-FTIR), and X-ray photoelectron spectroscopy (XPS). The protein-repelling and blood compatibility properties were evaluated, and separation of proteins was performed. We demonstrated that dynamic coatings based on the ionic complementary peptides provide an effective means for surface modification of PDMS-based microfluidic chips.

EXPERIMENTAL SECTION

Materials and Solutions. EAR16-II (>95% pure by high-pressure liquid chromatography) were synthesized by Karebay Corporation (Ningbo, China). Methylcellulose (MC), *n*-dodecyl-β-D-maltoside (DDM), sodium dodecyl sulfate (SDS), and *n*-dodecyltrimethylammonium chloride (DTAC) were purchased from Sigma-Aldrich (St. Louis, MO). FITC (fluorescein isothiocyanate)-BSA (bovine serum albumin), FITC-LYZ (lysozyme), FITC-fetuin, FITC-HSA (human serum albumin), FITC-Arg (arginine), and FITC-Phe (phenylalanine) were obtained from Zhongkechenyu Corporation (Beijing, China). PDMS base and curing agent (Sylgard 184 silicone elastomer kit) were purchased from Dow Corning (Midland, MI). Negative resist NR21-20000P, developer, and resist remover were purchased from Futurrex (Franklin, NJ). Blood used for the scanning electron microscopy experiment was drawn from a healthy person. All other chemicals were of analytical grade and purchased from local commercial suppliers. Deionized (DI) water (Milli-Q; Millipore, Bedford, MA) was used to prepare aqueous solutions.

A stock solution of 4.0 mg/mL EAR16-II was prepared in DI water. Coating buffers with 1.0 mg/mL EAR16-II were prepared by the dilution of the stock solution with a 10 mM phosphate (pH 9.5) containing 0.05% (w/v) MC, DDM, cellobiose, SDS, or DTAC.

Fabrication of Microchips. The PDMS microfluidic chips were fabricated in PDMS using a rapid prototyping technique,[9,17,32] starting with a master composed of a positive relief of negative NR21-20000P resist on a glass slide made by photolithography. PDMS base and curing agent with a mass ratio of 10:1 were mixed thoroughly, degassed under vacuum, poured onto the master, and cured in a vacuum oven at 70 °C for 90 min. Then the PDMS replica was peeled from the master, punched holes (2.5 mm in diameter) to create the reservoirs, and irreversibly bonded to a microscope glass slide using air plasma to form a PDMS/glass microchip with a simple cross channel of 100 μm width and 30 μm depth.

Surface Modification. PDMS surface specimens were prepared by a simple dipping and evaporation method. Cured PDMS slabs (10 mm × 10 mm × 2 mm) were first sonicated in 1.0 M NaOH and DI water three times for a total of 15 min and dried with nitrogen gas to obtain hydrophobic PDMS. The clean PDMS slabs were then treated in air plasma for 120 s using a PDC-32G plasma cleaner (Harrick Plasma, Pleasantville, NY) to obtain hydrophilic PDMS. Then, PDMS slabs were immediately immersed in coating buffers at room temperature for 30 s. Afterward, PDMS slabs were removed from the solution and dried under vacuum at room temperature. After washing with copious DI water and drying under vacuum at room temperature for 60 min, PDMS specimens were finally characterized by AFM, WCA, ATR-FTIR, and XPS measurements.

Surface Characterization of PDMS Specimens. The AFM images of native and EAR16-II-coated PDMS surfaces were acquired using a CSPM5500 atomic force microscope (AFM) (Beijing, China) in tapping mode. The measurements were performed at a scan frequency of 2 Hz using a standard silicon tip with a resonance frequency at 306 kHz. Measurements were made three times on different zones of each sample in a scanning area of 2.0 μm × 2.0 μm. Static contact angle measurements were performed on the specimens using an OCA 20 optical contact angle meter (Dataphysics, Inc., Stuttgart, Germany) via the sessile drop technique using DI water. Each data given was based on ten contact angle measurements at five different positions on the PDMS specimens. ATR-FTIR spectra were collected using a Tensor 27 infrared spectrometer (Bruker, Billerica, MA) with a wedged germanium crystal of attenuated total reflectance accessory. All spectra of the PDMS specimens were obtained at a 45° angle of incidence for 64 scans with a resolution of 4 cm^{-1} in the range of 400−4000 cm^{-1} at room temperature. XPS analyses were performed on an Axis Ultra X-ray photoelectron spectrometer (Kratos Analytical Ltd., Manchester, UK) with an Al X-ray source operating at 150 W (15 kV, 10 mA). The vacuum in the main chamber was kept above 3 × 10^{-9} Pa during XPS data acquisition. The specimens were analyzed at an electron take-off angle of 45° with respect to the surface plane. General survey scans (binding energy range 0−1200 eV, pass energy 80 eV) and high-resolution spectra (pass energy 75 eV) in the C 1s, O 1s, Si 2p, Si 2s, and N 1s regions were recorded for all modified PDMS substrates. The binding energies (BEs) were referenced to the C 1s binding energy at 284.6 eV.

Characterization of Biofouling Resistance and Protein Electrophoresis on Microchannels. Fluorescence microscopy measurements were used to evaluate nonspecific protein adsorption on microchannels. Protein adsorption assay was performed similar to the method previously reported.[17] The fluorescence images of the channel surfaces were recorded using an inverted microscope (Olympus IX51, Tokyo, Japan) with a CCD camera (QIMAGING, Micropublisher 5.0 RTV).

Scanning electron microscopy (SEM) was used to test the platelet adhesion on PDMS surfaces from plasma. Blood (4.5 mL) was

DOI: 10.1021/acs.langmuir.5b01085
Langmuir 2015, 31, 5891−5898

collected from a healthy person in a local hospital using the standard procedure into a PET tube containing 3.8 wt % citrate sodium solution (0.5 mL) as anticoagulant. Platelet-rich plasma (PRP) was obtained by centrifugation of the anticoagulated blood at 1200 rpm for 15 min. Then, the coated and uncoated PDMS substrates were incubated in PRP for 2 h at 37 °C. After being washed with PBS (20 mM, pH 7.4) three times, the substrates were immersed into 2.5% (v/v) glutaraldehyde solution for 30 min to fix the adhered platelet. The samples were air-dried and sputter-coated using gold prior to observation under Quanta 200 scanning electron microscope (FEI, Portland, OR). Thrombus accumulation was performed with *in vitro* blood flow model.[18] Uncoated and coated PDMS-based microchannels were subject to whole blood flow, and each experiment process lasted 30 min with 500 μL of human whole blood. Then the microchannels were rinsed with copious PBS and dried in air. The images of PDMS-based microfluidic chips were recorded with a CCD camera.

Microchip electrophoresis of samples was carried out using a laboratory-built system based on an Olympus IX51 inverted fluorescence microscope with a 100 W high-pressure mercury lamp as excitation radiation coupled with a Model N2000 chromatography workstation (Zhejiang University, Hangzhou, China) for data acquisition. Voltages to reservoirs adjustable in the range of −1.5 to +1.5 kV were provided by a HVS448-3000D high-voltage sequencer (LabSmith, Livermore, CA). FITC-labeled samples were separated at a field strength of 270 V/cm using the EAR16-II-coated PDMS microchannels.

Safety Considerations. The MCE used high voltage; hence, special care should be taken when handling the electrophoresis electrodes to avoid possible electrical shock.

RESULTS AND DISCUSSION

Characterization of EAR16-II Coatings on PDMS Surfaces. Nonspecific protein fouling represents one of the most encountered and challenging problem in PDMS-based microfluidic chips. Proteins in biological samples strongly interact with the PDMS surface via various noncovalent interactions, generally a combination of van der Waals, hydrophobic, hydrogen bonds, electrostatic, and salt bridges forces. Current coating additives such as surfactants and water-soluble polymers extensively used for surface modification of PDMS-based microfluidic chips, which do not have versatile structural and functional groups and multimolecular interactions involved in proteins, have shown very limited success in suppressing nonspecific protein adsorption. On the other hand, peptides with carefully tailored amino acid composition and sequence may show stronger surface binding affinity than proteins since peptide molecules strongly interact with the PDMS surface via the same noncovalent forces as proteins but with more favorable intermolecular interactions derived from highly ordered and tight self-assembling. To verify our hypothesis, we first performed MCE of FITC-Arg and FITC-Phe using EAR16-II as a dynamic coating additive. As shown in Figure 1A, no reproducible separation of FITC-Arg and FITC-Phe was obtained in an uncoated microchannel due to strong adsorption of analytes on the channel wall. In contrast, concentrations of EAR16-II above 1.0 mg/mL in running buffers greatly suppressed nonspecific adsorption of analytes and EOF and allowed reproducible separations. The EOF of a 10 mM phosphate buffer (pH 9.5) reduced from (4.2 ± 0.12) × 10^{-4} cm^2 V^{-1} s^{-1} (n = 4) in a native PDMS channel to (0.44 ± 0.06) × 10^{-4}, (0.42 ± 0.04) × 10^{-4}, and (0.39 ± 0.03) × 10^{-4} cm^2 V^{-1} s^{-1} (n = 4) in EAR16-II, EAR16-II/MC, and EAR16-II/DDM-coated PDMS channels, respectively, and the direction of EOF was from anode to cathode. The relative standard deviation (RSD) values of the migration times of 1.3%

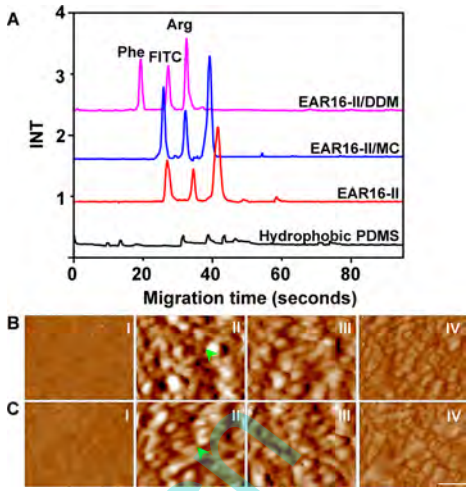

Figure 1. (A) Microchip electropherograms of FITC-Arg and FITC-Phe on native hydrophobic PDMS microchannels dynamically coated with 1.0 mg/mL EAR16-II/0.05% DDM, 1.0 mg/mL EAR16-II/0.05% MC, 1.0 mg/mL EAR16-II, and 0.0 mg/mL EAR16-II. Conditions: 10 mM phosphate buffer, pH 9.5, the effective separation length of 25 mm, and E_{sep} = 270 V/cm. AFM topography images (2 μm × 2 μm) of (B) the native hydrophobic PDMS and (C) the plasma-oxidized hydrophilic PDMS surfaces. The uncoated PDMS (BI, CI) and coated PDMS by EAR16-II (BII, CII), EAR16-II/MC (BIII, CIII), and EAR16-II/DDM (BIV, CIV). Scale bar: 500 nm.

and 1.9% and the theoretical plates of about 0.84 × 10^5 and 1.06 × 10^5 plates/m were obtained for FITC-Phe and FITC-Arg, respectively (the red line in Figure 1A, data obtained in independent separations on four channels, n = 4). These results clearly indicate that EAR16-II can readily form a coating layer on the channel wall, which significantly suppresses nonspecific adsorption of analytes and improves the separation performance of PDMS-based microfluidic chips. Next, we investigated effect of various surfactants including SDS, DTAC, DDM, and MC on the performance of EAR16-II coating on PDMS microchannels. Among them, MC and DDM as low as 0.05% (w/v) in the running buffer further improve the separation performance of FITC-Arg and FITC-Phe, leading to ∼3 and ∼8 s decreases in migration time, 25.9% and 32.8% reductions in the RSD value of migration time (n = 4), and ∼98.6% and ∼114.9% increases in theoretical plate, respectively (Supporting Information, Table S1). However, no noticeable improvement in separation performance was observed with SDS and DTAC even at high concentrations. DDM shares the common glucose residues with MC and the same alkyl chain with SDS and DTAC in structure. Therefore, these results strongly imply that the saccharide moiety of DDM and MC plays an important role in EAR16-II assembling on PDMS surfaces. Because PDMS-based microfluidic chips are most fabricated by irreversibly bonding a PDMS chip replica into a PDMS slab or a glass slide via plasma-oxidized surface activation, we subsequently characterized the EAR16-II self-assembling on native hydrophobic and plasma-oxidized hydrophilic PDMS surfaces.

AFM measurements confirm the existence of self-assembled EAR16-II films that are irreversibly adsorbed onto the PDMS surfaces intact by rising with copious water or buffer. Figures 1B and 1C show the AFM images of uncoated and EAR16-II-coated PDMS surfaces. Hydrophobic and hydrophilic PDMS surfaces looked smooth with discernible ridge and valley structures (Figures 1BI and 1CI). After EAR16-II modification,

DOI: 10.1021/acs.langmuir.5b01085
Langmuir 2015, 31, 5891−5898

almost identical topography changes were observed on both hydrophobic and hydrophilic PDMS surfaces. EAR16-II self-organized into orderly ribbon-like nanostructures (arrows in Figures 1BII and 1CII), forming thicker and continuous films with various uncovered holes. In the presence of MC, similarly thicker and continuous films with fewer uncovered valleys were assembled onto the PDMS surfaces (Figures 1BIII and 1CIII). When DDM was used, EAR16-II self-organized into nearly complete and compact films primarily composed of more tightly packed EAR16-II assemblies on both hydrophobic and hydrophilic PDMS surfaces (Figures 1BIV and 1CIV). The nearly identical topographies of EAR16-II-coated surfaces strongly suggest that the self-assembled EAR16-II films under the same conditions might have a similar secondary structure and coverage on both hydrophobic and hydrophilic PDMS surfaces.

Static WCA measurements were employed to monitor the surface characteristics of EAR16-II-coated PDMS substrates. For comparison, uncoated hydrophobic and hydrophilic PDMS substrates served as the controls. As shown in Table 1, EAR16-II-coated hydrophobic PDMS exhibited a mild decrease in WCAs from 120.3° ± 0.6 to 106.7° ± 0.6, whereas EAR16-II-coated hydrophilic PDMS showed a remarkable increase in WCAs from 12.5° ± 0.3 to 106.4° ± 0.4 with a stable nature in air for at least 2 weeks. These WCA data confirm the AFM observations of self-assembled EAR16-II amphipathic films on both hydrophobic and hydrophilic surfaces. Since the hydrophobic sides of amphipathic films of peptides and proteins generally show WCAs larger than 100°,[33] these comparably WCAs of EAR16-II amphipathic films strongly suggest that EAR16-II molecules were oriented correctly with their hydrophobic sides exposed to the solution. These results thus suggest a key role of electrostatic and H-bonding interactions rather than hydrophobic interaction for the spontaneous adsorption of peptides on both hydrophobic and hydrophilic PDMS surfaces. Low concentrations of MC slightly increased WCAs to 108.9 ± 0.5° and 108.2 ± 0.8° on EAR16-II-coated hydrophobic and hydrophilic PDMS surfaces, respectively; DDM further increased WCAs to 111.1 ± 0.6° and 111.3 ± 0.3°, respectively. On the other hand, DDM coating alone resulted in WCAs of 113.5 ± 0.5° and 111.7 ± 0.8° while MC coating yielded WCAs of 72.4 ± 0.7° and 71.2 ± 0.5° on hydrophobic and hydrophilic PDMS surfaces, respectively (Supporting Information, Table S2). These results rule out the hybrid assembly of EAR16-II with MC or DDM and accordingly indicate that DDM and MC greatly promote EAR16-II assembly on PDMS surfaces. Notably, EAR16-II yielded very comparable WCAs under the same condition, suggesting again that the self-assembled EAR16-II amphipathic films should have similar secondary structure and coverage on both hydrophobic and hydrophilic PDMS surfaces.

Table 1. Water Contact Angles on PDMS Surfaces Coated with EAR16-II, EAR16-II/MC, and EAR16-II/DDM

	WCAs[a] (deg)	
coating additives	hydrophobic PDMS	hydrophilic PDMS
no additives	120.3 ± 0.6	12.5 ± 0.3[b]
1.0 mg/mL EAR16-II	106.7 ± 0.6	106.4 ± 0.4
1.0 mg/mL EAR16-II/0.05% MC	108.9 ± 0.5	108.2 ± 0.8
1.0 mg/mL EAR16-II/0.05% DDM	111.1 ± 0.6	111.3 ± 0.3

[a]Data are reported as the mean ± standard error (n = 6). [b]WCAs were collected within ~10 min after air plasma treatment.

ATR-FTIR spectroscopy was performed to further investigate the secondary structure of the self-assembled EAR16-II amphipathic films and provide new insights with respect to the AFM and WCA data. The amide I band at 1600−1700 cm^{-1}, formed largely due to the C═O stretching vibration of the peptide amide bond and highly sensitive to the secondary structure of the peptide backbone, has been widely used for conformational studies.[26−29] As shown in Figures 2A and 2B,

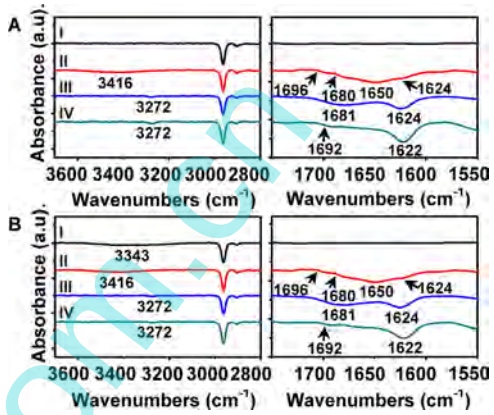

Figure 2. ATR-FTIR spectra of (A) the hydrophobic PDMS and (B) hydrophilic PDMS surfaces. The uncoated PDMS (AI, BI) and the coated PDMS by EAR16-II (AII, BII), EAR16-II/MC (AIII, BIII), and EAR16-II/DDM (AIV, BIV).

the broad OH and NH bands and the amide I bands were observed in the range of 3200−3600 and 1600−1700 cm^{-1}, respectively, on all EAR16-II-coated PDMS surfaces, confirming the existence of the self-assembled EAR16-II amphipathic films as observed by AFM and WCAs measurements. The broad bands centered at 1650 cm^{-1} were attributed to α-helix and random coil structures, whereas those at 1624 and 1696 cm^{-1} were ascribed to β-sheet structures. The shoulder bands at 1680 cm^{-1} were attributed to β-turn structures (Figures 2AII and 2BII).[26,27,34,35] Hence, EAR16-II assembles onto the both hydrophobic and hydrophilic PDMS surfaces with a mixture of α-helices, β-sheets, β-turns, and random coils, which is similar to what was observed in solution by circular dichroism spectroscopy (CD) (Supporting Information, Figure S1 and Table S3). In the presence of MC, two prominent peaks at 1624 and 1681 cm^{-1} that are characteristic of β-sheet structures were observed for EAR16-II on the hydrophobic and hydrophilic PDMS surfaces (Figures 2AIII and 2BIII). The large peaks at 1681 cm^{-1} arise from a mixture of the β-turn and β-sheet structures. In particular, the characteristic peaks of α-helix and random coil structures at 1650 cm^{-1} disappeared entirely. In the presence of DDM, the spectra of the amide I band for EAR16-II are essentially identical on both PDMS surfaces (Figures 2AIV and 2BIV). An intense and narrow band at 1622 cm^{-1} and a weak band at 1692 cm^{-1} are indicative of tightly packed β-sheets, which contribute a predominant portion of the secondary structure (Figures 2AIV and 2BIV).[26,34,35] The weak and broad absorption at 1662−1686 cm^{-1} in EAR16-II/DDM suggests that β-turn structures still account for a small portion of the secondary structure. On the other hand, no noticeable change in conformation was observed with SDS and DTAC (Supporting Information,

DOI: 10.1021/acs.langmuir.5b01085
Langmuir 2015, 31, 5891−5898

Figure S2). These results strongly suggest again that the saccharide moiety of DDM and MC mediate EAR16-II assembly onto PDMS surfaces. If this is true, simple carbohydrates such as cellobiose should also yield an evident change in conformation. Indeed, a narrow and intense band at 1622 cm^{-1} coupled with a weak band at 1692 cm^{-1} was observed for EAR16-II/cellobiose (Supporting Information, Figure S2AV, BV), undoubtedly revealing a key role of carbohydrates in mediating the peptide assembly onto the PDMS surfaces.

We also recorded the ATR-FTIR spectra of DDM-, MC-, and cellobiose-coated PDMS surfaces to further assess whether carbohydrate derivatives coassembled with EAR16-II (Supporting Information, Figure S3). The typical absorption bands of these carbohydrate derivatives, such as CH stretching vibrations at 2830−2998 cm^{-1} and the CH bending vibrations at 1346−1500 cm^{-1} (Supporting Information, Figure S3), were not observed in Figures 2A and 2B, thus indicating the nonexistence of MC, DDM, and cellobiose in the self-assembled EAR16-II amphipathic films on the PDMS surfaces. MC, DDM, and cellobiose, which share common glucose residues with multiple hydroxyl groups in structure, can form complexes with peptides via hydrogen bonding and other weak forces in solution. Such peptide−carbohydrate complexes bring the peptide molecules together at the water−PDMS interfaces, thus promoting the formation of β-sheets. Based on the ratio of the 1622−1624 and the 1662−1686 cm^{-1} peak heights, the relative content of β-sheet structures formed in the presence of carbohydrate derivatives can be estimated and follows this order: DDM > cellobiose ≫ MC. The DDM and cellobiose are apparently more effective than MC in promoting formation of β-sheets while excluding other secondary structures. MC consists of linear polysaccharides with ∼450 $\beta(1-4)$-linked glucose residues on an average, whereas DDM and cellobiose have two $\beta(1-4)$-linked and $\alpha(1-4)$-linked glucose residues in their structure, respectively. Therefore, large differences in promoting formation of β-sheets observed for MC, cellobiose, and DDM should arise from steric hindrance rather than the conformation of carbohydrates. In summary, the ATR-FTIR spectra provided strong support for the AFM and WCA observations that EAR16-II assemblies have similar secondary structure on both hydrophobic and hydrophilic PDMS surfaces.

The surface chemical compositions of the uncoated and EAR16-II-coated PDMS surfaces were determined by XPS. The XPS spectra of uncoated hydrophobic and hydrophilic PDMS substrates showed four typical peaks: O 1s, C 1s, Si 2s, and Si 2p at 531, 283, 151, and 102 eV, respectively (Figure 3). The

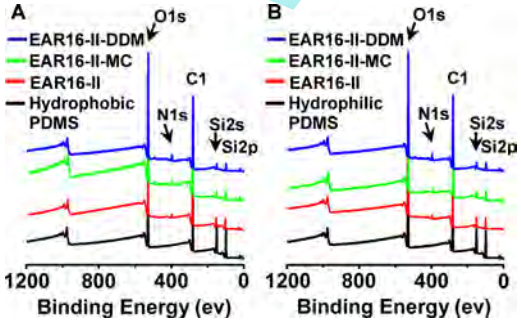

Figure 3. XPS spectra of (A) the uncoated and EAR16-II-coated hydrophobic PDMS surfaces and (B) the uncoated and EAR16-II-coated hydrophilic PDMS surfaces.

air plasma treatment led to a remarkable increase in the oxygen peak and a decrease in the carbon peak, whereas the silicon peaks decreased only slightly—a finding comparable to those of previous studies.[36,37] Hydrophobic PDMS substrates exhibited a ratio of 0.51 between the O 1s and C 1s photoemissions, whereas hydrophilic PDMS substrates became oxygen-rich with a O 1s:C 1s ratio of 1.24 (Supporting Information, Table S4) after the plasma treatment. This was due to the formation of hydroxyl, carboxyl, and peroxide functionalities on the surface. The N 1s peak at 398 eV appeared only after EAR16-II modification, and the dramatic decrease of Si 2s and Si 2p peaks is indicative of the self-assembled EAR16-II amphipathic films on PDMS surfaces. As expected, the carbohydrate derivatives further increased the N 1s signals and decreased the Si 2s and Si 2p signals in the order DDM > MC > EAR16-II. The element Si belongs only to PDMS surfaces, whereas the element N exists only in the amine groups of EAR16-II. Therefore, the gradual increase in the nitrogen (N) content coupled with the progressive decrease in silicon (Si) content in the presence of MC and DDM indicated that EAR16-II has been steadily covered PDMS surfaces to a great extent. Notably, the atomic concentrations were quite comparable under the same conditions (Supporting Information, Table S4), thereby confirming the similar coverage of EAR16-II assemblies on both hydrophobic and hydrophilic PDMS surfaces.

In summary, β-sheet amphipathic films with similar secondary structure and coverage by carbohydrate-mediated self-assembly of EAR16-II on both hydrophobic and hydrophilic PDMS surfaces were confirmed using AFM, WCA, ATR-FTIR, and XPS experiments, thus suggesting the same mechanism of peptide adsorption on the PDMS surfaces.

Characterization of Nonspecific Protein Adsorption and Protein Separation on EAR16-II-Coated PDMS Channels. BSA and LYZ were chosen as model proteins to evaluate the effect of self-assembled EAR16-II amphipathic films for suppressing nonspecific protein adsorption onto the PDMS surfaces. The protein repelling study of each microchannel was performed by first filling the microchannel with a solution of 1.0 mg/mL FITC-BSA or FITC-LYZ in a 20 mM PBS (pH 7.4) and maintaining it at 37 °C for 1 h. The resulting protein contaminated microchannels were thoroughly cleaned with a 20 mM PBS solution (pH 7.4). Finally, the nonspecific adsorption of FITC-BSA and FITC-LYZ was quantified by fluorescence microscopy (Supporting Information, Figure S4). At a pH 7.4, BSA (pI 4.7) and LYZ (pI 11) are negatively and positively charged, respectively, while hydrophobic and hydrophilic PDMS surfaces are negatively charged. However, the fluorescence images indicate that FITC-BSA and FITC-LYZ adsorbed strongly onto the surfaces of the hydrophobic and hydrophilic PDMS microchannels, suggesting a key role of hydrogen bonds and salt bridges forces in spontaneous adsorption of proteins at solid surfaces. On the contrary, the adsorption of FITC-BSA and FITC-LYZ was significantly minimized on EAR16-II-coated channel surfaces. The quantitative amounts of protein adsorbed onto uncoated and EAR16-II-coated PDMS microchannels are shown in Figure 4A. On the hydrophobic PDMS surface, EAR16-II, EAR16-II/MC, and EAR16-II/DDM coatings led to 97.3%, 97.7%, and 98.2% reductions in BSA adsorption and to 96.7%, 97.3%, and 98.0% reductions in LYZ adsorption, respectively. On the hydrophilic PDMS surface, EAR16-II, EAR16-II/MC, and EAR16-II/DDM coatings led to 97.3%, 97.6%, and 98.3% reductions in BSA adsorption and to 96.8%, 97.2%, and 98.1% reductions in LYZ

DOI: 10.1021/acs.langmuir.5b01085
Langmuir 2015, 31, 5891−5898

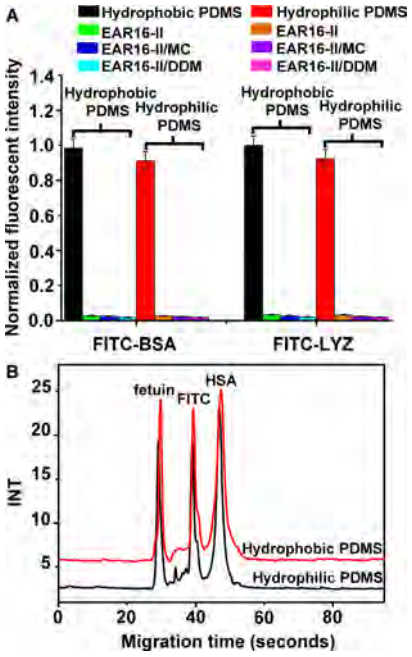

Figure 4. (A) Adsorption of FITC-BSA and FITC-LYZ on the hydrophobic and hydrophilic PDMS microchannels, which correspond to the fluorescent micrographs in Supporting Information Figure S4A,B. Data are expressed as mean ± SD (n = 6). (B) Microchip electropherograms of FITC-fetuin and FITC-HSA on the hydrophobic and hydrophilic PDMS microchannels coated with 1.0 mg/mL EAR16-II and 0.05% DDM. Conditions: E_{sep} = 270 V/cm; 10 mM phosphate buffer, pH 9.5, and the effective separation length of 25 mm.

adsorption, respectively, which are better than or comparable to most chemical modifications.[16,17] In addition, the protein-repelling capability of EAR16-II coatings followed the order of DDM > MC > EAR16-II, which again is in good agreement with AFM, WCA, ATR-FTIR, and XPS observations that more tightly packed β-sheets result in more protein-repelling surfaces. The EAR16-II amphipathic films composed of tightly packed β-sheet assemblies exhibited excellent protein-repelling properties to both positively and negatively charged proteins, holding great potential for applications involved in complex media, such as blood serum or plasma.

Figure 4B shows the microchip electropherograms of FITC-fetuin and FITC-HSA on the EAR16-II/DDM-coated PDMS microchannels. The hydrophobic and hydrophilic PDMS microchannels were modified first by flushing the channel with 100 μL of a 10 mM phosphate buffer (pH 9.5) containing 1.0 mg/mL EAR16-II and 0.05% (w/v) DDM and then rinsing the microchannel with 100 μL of a 10 mM phosphate buffer (pH 9.5). Prior to separation, the microchannels were filled with a 10 mM phosphate buffer (pH 9.5) without any additives. FITC-fetuin and FITC-HSA were well separated in a 2.5 cm microchannel within 50 s with high efficiency and reproducibility. Theoretical plates of about 1.94×10^5 and 1.56×10^5 plates/m for FITC-fetuin and 1.02×10^5 and 1.51×10^5 plates/m for FITC-HSA were obtained on EAR16-II-coated hydrophobic and hydrophilic PDMS microchannels, respectively. The RSD values of the migration times were less than 1.6% and 1.9%, respectively, on four different EAR16-II-coated hydrophobic and hydrophilic PDMS microchannels. The separations of proteins are comparable to those obtained by chemical modified PDMS microchannels,[19,20] further verifying the negligible nonspecific adsorption of proteins on EAR16-II-coated PDMS microchannels.

Blood Compatibility of EAR16-II-Coated PDMS Microchannels. PDMS-based microfluidic chips have been extensively used for various biological and biomedical applications. In the case of whole blood contacting applications, circulating plasma proteins tend to absorb instantaneously onto the surface of microchannels, which in turn results in platelet adhesion and activation, thrombus formation, and ultimately device failure. Therefore, it is important to fabricate a surface that might prevent the adsorption of proteins, peptides, or other biomolecules in more complex media such as blood serum, plasma, or whole blood. The uncoated and EAR16-II-coated PDMS microchannels were tested after exposure to the healthy human platelet-rich plasma and whole blood samples, respectively. SEM images in Figure 5A showed that the

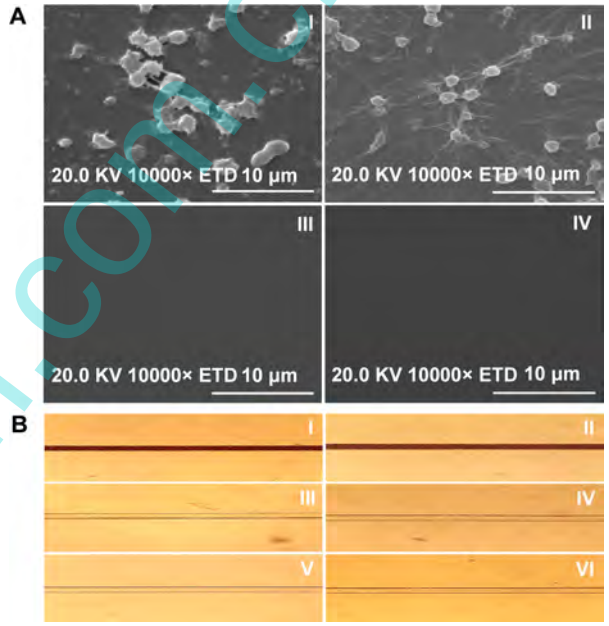

Figure 5. (A) SEM images of (left) the hydrophobic PDMS and (right) hydrophilic PDMS surfaces after exposure in healthy human plasma. (B) Optical photos of (left) the hydrophobic PDMS and (right) hydrophilic PDMS microchannels from whole blood flow tests. The uncoated PDMS (I, II) and coated PDMS by EAR16-II/DDM (III, IV). The uncoated control PDMS channels rinsed by PBS (V, VI).

adsorption of platelets on the EAR16-II-coated PDMS surfaces was obviously suppressed as compared with the uncoated ones. These results are comparable to the previous reports[18,38] and coincide well with the fact that the EAR16-II-coating efficiently alleviates protein adsorption on the PDMS surfaces. Furthermore, whole blood flow testing showed that the blood coagulation and thrombus formation are observed in the uncoated PDMS microchannels of 100 μm width and 30 μm depth in ~30 min, causing significant occlusion of the channels (Figures 5BI and 5BII). By comparison, EAR16-II coated PDMS microchannels exhibited a clean channel surface devoid of major thrombus (Figures 5BIII and 5BIV) similar to the uncoated control microchannels rinsed by PBS (Figures 5BV and 5BVI), respectively. The excellent platelet- and thrombus-resistant properties of the EAR16-II coating match well with actual applications for minimizing the surface fouling of

DOI: 10.1021/acs.langmuir.5b01085
Langmuir 2015, 31, 5891−5898

microfluidic devices by biological species in whole blood, especially in an extracorporeal or *in vivo* environment.

On the basis of the aforementioned study and the well-characterized structure of β-sheets, we draw a schematic model to explain the interactions of EAR16-II with the PDMS surfaces and the antifouling capability of EAR16-II coatings at a molecular level (TOC graphic). Low concentration of carbohydrates may form complexes with EAR16-II in solution via hydrogen bonding and other interactions. The EAR16-II/carbohydrate complexes bring the peptide molecules to the water-PDMS interfaces and promote formation of tightly packed β-sheets, yielding a nearly complete and compact amphipathic film on both hydrophobic and hydrophilic PDMS surfaces. The hydrophilic side and hydrophobic side of the amphipathic film exposed to the surface and to the solution, respectively. It should be noted that the assembly of EAR16-II on the PDMS surfaces might be parallel or antiparallel and with various position shifts between peptides. Because both native hydrophobic and plasma-oxidized hydrophilic PDMS surfaces as well as EAR16-II are negatively charged at pH 9.5, these results strongly suggest that the interactions between the guanidine groups of EAR16-II and the surface negative charges, i.e., strong ionic hydrogen bonds,[39] play a key role in the adsorption of peptides on PDMS surfaces. The detailed mechanism is under investigation. In other words, the spontaneous adsorption of EAR16-II from solution onto the PDMS surface should mostly arise from the surface negative charges rather than the hydrophobicity of PDMS. On the other hand, the hydrophilic side of the EAR16-II amphipathic films facing to the surface clearly indicate that EAR16-II do interact with the PDMS surfaces via a combination of various noncovalent interactions such as van der Waals, hydrophobic, hydrogen bonds, electrostatic, and salt bridge forces in the same way as proteins. However, tightly packed EAR16-II in β-sheets allows more favorable intermolecular interactions including hydrogen bonds, hydrophobic, and van der Waals forces than proteins. As a result, the adsorption of EAR16-II on the PDMS surfaces is more energetically favorable than that of proteins in general, so that proteins are failed to substitute EAR16-II to contaminate the PDMS surface. In addition, the fact that the hydrophobic side of amphipathic film exposed to the solution means that proteins interact with the EAR16-II-coated PDMS surfaces primarily via van der Waals, hydrophobic, and other weak forces. This is another key factor for the EAR16-II coating to minimize the nonspecific protein adsorption on the PDMS surfaces.

CONCLUSION

In the current work, the EAR16-II self-assembling on both native hydrophobic and plasma-oxidized hydrophilic PDMS surfaces was comprehensively investigated. We first demonstrate that EAR16-II can readily self-assemble into amphipathic films primarily composed of tightly packed β-sheets in the presence of carbohydrate derivatives on the PDMS surfaces. The self-assembled EAR16-II amphipathic film exhibits excellent protein-repelling and blood compatibility properties resulted from the same interactions with the surface as proteins but more favorable intermolecular interactions of peptide molecules. A schematic model has been proposed to explain the interactions of EAR16-II with the PDMS surface and the antifouling capability of EAR16-II coatings at a molecular level. Considering its remarkable simplicity, efficiency, and flexibility to irregular surfaces in large scale as well as the easy synthesis and diverse structure of peptides, the surface modification based on self-assembling peptides will provide a novel approach to address the nonspecific protein fouling and biocompatibility of PDMS-based microfluidic chips that can facilitate potential uses in clinical diagnostics, high-throughput screening, biosensing, and proteomics applications.

ASSOCIATED CONTENT

Supporting Information

Figures S1−S4 and Tables S1−S4. The Supporting Information is available free of charge on the ACS Publications website at DOI: 10.1021/acs.langmuir.5b01085.

AUTHOR INFORMATION

Corresponding Author

*E-mail dangfqn@snnu.edu.cn; Fax (+86) 29-8153-0727 (F.D.).

Notes

The authors declare no competing financial interest.

ACKNOWLEDGMENTS

This work was supported by the National Natural Science Foundation of China (No. 21175088).

REFERENCES

(1) Mcdonald, J. C.; Whitesides, G. M. Poly(dimethylsiloxane) as a Material for Fabricating Microfluidic Devices. *Acc. Chem. Res.* **2002**, *35*, 491−499.

(2) Berthier, E.; Young, E. W. K.; Beebe, D. Engineers are from PDMS-land, Biologists are from Polystyrenia. *Lab Chip* **2012**, *12*, 1224−1237.

(3) Nge, P. N.; Rogers, C. I.; Woolley, A. T. Advances in Microfluidic Materials, Functions, Integration, and Applications. *Chem. Rev.* **2013**, *113*, 2550−2583.

(4) Ren, K.; Zhou, J.; Wu, H. Materials for Microfluidic Chip Fabrication. *Acc. Chem. Res.* **2013**, *46*, 2396−2406.

(5) Zhang, R.; Gong, H.; Zeng, X. D.; Sze, C. C. A High-Throughput Microfluidic Biochip to Quantify Bacterial Adhesion to Single Host Cells by Real-Time PCR Assay. *Anal. Bioanal. Chem.* **2013**, *405*, 4277−4282.

(6) Fan, H. C.; Gu, W.; Wang, J.; Blumenfeld, Y. J.; El-Sayed, Y. Y.; Quake, S. R. Non-invasive Prenatal Measurement of the Fetal Genome. *Nature* **2012**, *487*, 320−324.

(7) Kemna, E. W. M.; Schoeman, R. M.; Wolbers, F.; Vermes, I.; Weitz, D. A.; van den Berg, A. High-Yield Cell Ordering and Deterministic Cell-in-Droplet Encapsulation Using Dean Flow in a Curved Microchannel. *Lab Chip* **2012**, *12*, 2881−2887.

(8) Croushore, C. A.; Supharoek, S.; Lee, C. Y.; Jakmunee, J.; Sweedler, J. V. Microfluidic Device for the Selective Chemical Stimulation of Neurons and Characterization of Peptide Release with Mass Spectrometry. *Anal. Chem.* **2012**, *84*, 9446−9452.

(9) Li, Y.; Liu, C.; Feng, X.; Xu, Y.; Liu, B. Ultrafast Microfluidic Mixer for Tracking the Early Folding Kinetics of Human Telomere G-Quadruplex. *Anal. Chem.* **2014**, *86*, 4333−4339.

(10) Carroll, M. J.; Stopfer, L. E.; Kreeger, P. K. A Simplified Culture System to Examine Soluble Factor Interactions between Mammalian Cells. *Chem. Commun.* **2014**, *50*, 5279−5281.

(11) Wong, I.; Ho, C. Surface Molecular Property Modifications for Poly(dimethylsiloxane) (PDMS) Based Microfluidic Devices. *Microfluid. Nanofluid.* **2009**, *7*, 291−306.

(12) Zhou, J.; Khodakov, D. A.; Ellis, A. V.; Voelcker, N. H. Surface Modification for PDMS-Based Microfluidic Devices. *Electrophoresis* **2012**, *33*, 89−104.

(13) Tran, N. T.; Ayed, I.; Pallandre, A.; Taverna, M.; Tran, N. T.; Ayed, I.; Pallandre, A.; Taverna, M. Recent Innovations in Protein

DOI: 10.1021/acs.langmuir.5b01085
Langmuir 2015, 31, 5891−5898

Separationon Microchips by Electrophoretic Methods: An Update. *Electrophoresis* **2010**, *31*, 147−173.
(14) Hoek, I.; Tho, F.; Arnold, W. M. Sodium Hydroxide Treatment of PDMS Based Microfluidic Devices. *Lab Chip* **2010**, *10*, 2283−2285.
(15) Zhou, J.; Ellis, A. V.; Voelcker, N. H. Recent Developments in PDMS Surface Modification for Microfluidic Devices. *Electrophoresis* **2010**, *31*, 2−16.
(16) Peng, X.; Zhao, L.; Du, G.; Wei, X.; Guo, J.; Wang, X.; Guo, G.; Pu, Q. Charge Tunable Zwitterionic Polyampholyte Layers Formed in Cyclic Olefin Copolymer Microchannels through Photochemical Graft Polymerization. *ACS Appl. Mater. Interfaces* **2013**, *5*, 1017−1023.
(17) Yang, L.; Li, L.; Tu, Q.; Ren, L.; Zhang, Y.; Wang, X.; Zhang, Z.; Liu, W.; Xin, L.; Wang, J. Photocatalyzed Surface Modification of Poly(dimethylsiloxane) with Polysaccharides and Assay of Their Protein Adsorption and Cytocompatibility. *Anal. Chem.* **2010**, *82*, 6430−6439.
(18) Zhang, Z.; Borenstein, J.; Guiney, L.; Miller, R.; Sukavaneshvar, S.; Loose, C. Polybetaine Modification of PDMS Microfluidic Devices to Resist Thrombus Formation in Whole Blood. *Lab Chip* **2013**, *13*, 1963−1968.
(19) Xiao, D.; Le, T. V.; Wirth, M. J. Surface Modification of the Channels of Poly(dimethylsiloxane) Microfluidic Chips with Polyacrylamide for Fast Electrophoretic Separations of Proteins. *Anal. Chem.* **2004**, *76*, 2055−2061.
(20) Makamba, H.; Hsieh, Y.-Y.; Sung, W.-C.; Chen, S.-H. Stable Permanently Hydrophilic Protein-Resistant Thin-Film Coatings on Poly(dimethylsiloxane) Substrates by Electrostatic Self-Assembly and Chemical Cross-Linking. *Anal. Chem.* **2005**, *77*, 3971−3978.
(21) Viefhues, M.; Manchanda, S.; Chao, T.-C.; Anselmetti, D.; Regtmeier, J.; Ros, A. Physisorbed Surface Coatings for Poly-(dimethylsiloxane) and Quartz Microfluidic Devices. *Anal. Bioanal. Chem.* **2011**, *401*, 2113−2122.
(22) Dang, F.; Maeda, E.; Osafune, T.; Nakajima, K.; Kakehi, K.; Ishikawa, M.; Baba, Y. Carbohydrate Protein Interactions Investigated on Plastic Chips Statically Coated with Hydrophobically Modified Hydroxyethylcellulose. *Anal. Chem.* **2009**, *81*, 10055−10060.
(23) Dang, F.; Hasegawa, T.; Biju, V.; Ishikawa, M.; Kaji, N.; Yasui, T.; Baba, Y. Spontaneous Adsorption on a Hydrophobic Surface Governed by Hydrogen Bonding. *Langmuir* **2009**, *25*, 9296−9301.
(24) Huang, B.; Wu, H.; Kim, S.; Zare, R. N. Coating of Poly(dimethylsiloxane) with *n*-Dodecyl-*β*-D-maltoside to Minimize Nonspecific Protein Adsorption. *Lab Chip* **2005**, *5*, 1005−1007.
(25) Larson, B. J.; Gillmor, S. D.; Braun, J. M.; Cruz-Barba, L. E.; Savage, D. E.; Denes, F. S.; Lagally, M. G. Long-Term Reduction in Poly(dimethylsiloxane) Surface Hydrophobicity via Cold-Plasma Treatments. *Langmuir* **2013**, *29*, 12990−12996.
(26) Lee, N. R.; Bowerman, C. J.; Nilsson, B. L. Effects of Varied Sequence Pattern on the Self-Assembly of Amphipathic Peptides. *Biomacromolecules* **2013**, *14*, 3267−3277.
(27) Capes, J. S.; Kiley, P. J.; Windle, A. H. Investigating the Effect of pH on the Aggregation of Two Surfactant-Like Octapeptides. *Langmuir* **2010**, *26*, 5637−8562.
(28) Gelain, F.; Silva, D.; Caprini, A.; Taraballi, F.; Natalello, A.; Villa, O.; Nam, K. T.; Zuckermann, R. N.; Doglia, S. M.; Vescovi, A. BMHP1-Derived Self-Assembling Peptides: Hierarchically Assembled Structures with Self-Healing Propensity and Potential for Tissue Engineering Applications. *ACS Nano* **2011**, *5*, 1845−1859.
(29) Guilbaud, J. B.; Rochas, C.; Miller, A. F.; Saiani, A. Effect of Enzyme Concentration of the Morphology and Properties of Enzymatically Triggered Peptide Hydrogels. *Biomacromolecules* **2013**, *14*, 1403−1411.
(30) Zhang, S.; Holmes, T.; Lockshin, C.; Rich, A. Spontaneous Assembly of a Self-Complementary Oligopeptide to Form a Stable Macroscopic Membrane. *Proc. Natl. Acad. Sci. U. S. A.* **1993**, *90*, 3334−3338.
(31) Yang, H.; Fung, S.; Pritzker, M.; Chen, P. Surface-Assisted Assembly of an Ionic-Complementary Peptide: Controllable Growth of Nanofibers. *J. Am. Chem. Soc.* **2007**, *129*, 12200−12210.
(32) Ji, J.; Nie, L.; Li, Y.; Yang, P.; Liu, B. Simultaneous Online Enrichment and Identification of Trace Species Based on Microfluidic Droplets. *Anal. Chem.* **2013**, *85*, 9617−9622.
(33) Wösten, H. A. B.; de Vocht, M. L. Hydrophobins, the Fungal Coat Unraveled. *Biochim. Biophys. Acta* **2000**, *1469*, 79−86.
(34) Roach, P.; Farrar, D.; Perry, C. C. Interpretation of Protein Adsorption: Surface-Induced Conformational Changes. *J. Am. Chem. Soc.* **2005**, *127*, 8168−8173.
(35) Barth, A. Infrared Spectroscopy of Proteins. *Biochim. Biophys. Acta* **2007**, *1767*, 1073−1101.
(36) Donzel, C.; Geissler, M.; Bernard, A.; Wolf, H.; Michel, B.; Hilborn, J.; Delamarche, E. Hydrophilic Poly(dimethylsiloxane) Stamps for Microcontact Printing. *Adv. Mater.* **2001**, *13*, 1164−1167.
(37) Olander, B.; Wirsén, A.; Albertsson, A. Argon Microwave Plasma Treatment and Subsequent Hydrosilylation Grafting as a Way to Obtain Silicone Biomaterials with Well-Defined Surface Structures. *Biomacromolecules* **2002**, *3*, 505−510.
(38) Bi, H.; Zhong, W.; Meng, S.; Kong, J.; Yang, P.; Liu, B. Construction of a Biomimetic Surface on Microfluidic Chips for Biofouling Resistance. *Anal. Chem.* **2006**, *78*, 3399−3405.
(39) Meot-Ner, M. Update 1 of: Strong Ionic Hydrogen Bonds. *Chem. Rev.* **2012**, *112*, PR22−PR103.

DOI: 10.1021/acs.langmuir.5b01085
Langmuir 2015, 31, 5891−5898